International Conference on Space Optics—ICSO 2022

Dubrovnik, Croatia

3–7 October 2022

Edited by Kyriaki Minoglou, Nikos Karafolas, and Bruno Cugny,

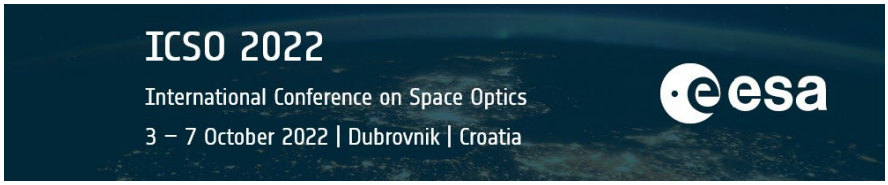

Technological innovation for the ALTIUS atmospheric limb sounding mission: steps towards flight

International Conference on Space Optics — ICSO 2022, edited by Kyriaki Minoglou, Nikos Karafolas, Bruno Cugny, Proc. of SPIE Vol. 12777, 127770I · © 2023 ESA and CNES · 0277-786X · doi: 10.1117/12.2688821

Technological innovation for the ALTIUS atmospheric limb sounding mission: steps towards flight

Saillen N[a], Aballea L[b], Buhler D[a], Montrone L[a], Navarro Reyes D[a], Francois M[a], Moelans W[b], Verstrynge T[b], Mollet D[b], Morel F[b], Pollier C[c], Naudet J[c], Dayers L[c], Famelaer A[c], Bouten J[c]
[a] ESA, Noordwijk , Netherlands
[b] OIP Sensor Systems N.V., Oudenaarde, Belgium
[c] QinetiQ Space N.V., Kruibeke, Belgium

ABSTRACT

The ALTIUS Mission (Atmospheric Limb Tracker for Investigation of the Upcoming Stratosphere) aims at the development of a limb sounder based on a small satellite concept to monitor the distribution and evolution of stratospheric ozone at high vertical resolution in support of operational services and long-term trend monitoring.

The ALTIUS instrument consists of three spectral imagers flying at an altitude of approximately 700 km Sun-Synchronous Orbit. The three hyperspectral channels are based on Acousto-Optic Tuneable Filters (AOTFs) in the Visible (440-675nm) and NIR (600-1020nm) range, and a cascade of Fabry-Pérot Interferometers (FPI) in the UV (250-355nm). The use of tuneable active spectral filters will allow the ALTIUS Instrument to perform observations with a spectral resolution ranging between 1nm and 10nm in an extremely versatile operational concept.

This paper presents the key technical challenges to be controlled on the design and technologies of the ALTIUS 2D imager for limb sounding. A particular insight will be given on its optical concept including the choice of tuneable spectral filters in each channel and the key development of optical elements such as mirrors, filters and coatings, ensuring the straylight performances of the instrument. The paper also provides a deep dive into the structural and thermal design of the instrument ensuring the pointing accuracy, and the way to achieve L1 radiometric performances from L0 instrument performances through calibration needs and data processing strategies. Along the lines, the stringent cleanliness and contamination control and related envisaged strategy to ensure sustained optical performances will be also described.

Keywords: European Space Agency, ALTIUS, limb, tuneable filters, AOTF, Fabry Perot Interferometer, Acousto-Optic Tuneable Filters, PROBA, Hyperspectral imager

1 INTRODUCTION

The ozone layer is a natural layer of gas in the upper atmosphere. Stratospheric ozone acts as sunscreen, absorbing much of the ultraviolet radiation in sunlight before it reaches Earth's surface – hence playing a vital role in protecting life on our planet.

While ozone depletion is not a major cause of climate change, the two are nevertheless linked. Ozone affects the temperature balance of Earth in two different ways. Firstly, it absorbs solar ultraviolet radiation, which heats the stratosphere. Secondly, it absorbs infrared radiation emitted by Earth's surface, effectively trapping heat in the troposphere.

Satellites orbiting above are the only way of measuring recovery and change in a consistent and systematic manner. However, most ozone-measuring satellites, such as the Copernicus Sentinel-5P mission, provide a value for the amount of ozone in a column – meaning the total amount of ozone in a column of air from the ground (or just above the ground) to the top of the atmosphere. In conjunction, profiles, which show concentrations at different altitudes, are also needed to gain the full picture. Since the end of ESA's Envisat mission, there are only a few instruments in orbit that provide profiles of ozone, and some of these missions will end in the next few years.

The ALTIUS mission, therefore, fills a very important gap in the continuation of 'limb' measurements for atmospheric science.

Proposed as an ESA Earth Watch mission in 2016, ALTIUS is funded mainly by Belgium with contributions from Canada, Luxembourg and Romania. The satellite is designed and built by a consortium of companies under the prime contractor QinetiQ Space in Belgium. OIP Sensor Systems is the prime contractor for the instrument. The ground segment for data processing is developed by a consortium under the prime contractor Spacebel in Belgium with scientific support from the Belgian Institute for Space Aeronomy (BISA) and the University of Saskatchewan (USASK) in Canada.

ALTIUS is scheduled to be launched in 2025 on a Vega-C rocket from Europe's Spaceport in Kourou, French Guiana.

1.1 Mission

The goal of the ALTIUS mission is to monitor the distribution and evolution of stratospheric ozone at high vertical resolution in support of operational services and long-term trend monitoring. It will provide detailed stratospheric profile information at high vertical resolution, which is a valuable addition to ozone total column for data assimilation systems based on nadir sounders used by operational centres. In addition, some secondary scientific mission objectives are targeted, including measurements of vertical concentration profiles of other atmospheric species.

In order to provide near global coverage of the ozone concentration. The ALTIUS mission will accommodate three observation modes: bright limb, Solar occultation and stellar occultation. In bright limb mode, the instrument will image the light scattered by the atmosphere. In solar and stellar occultation, it will image the Sun or star going through the atmosphere.

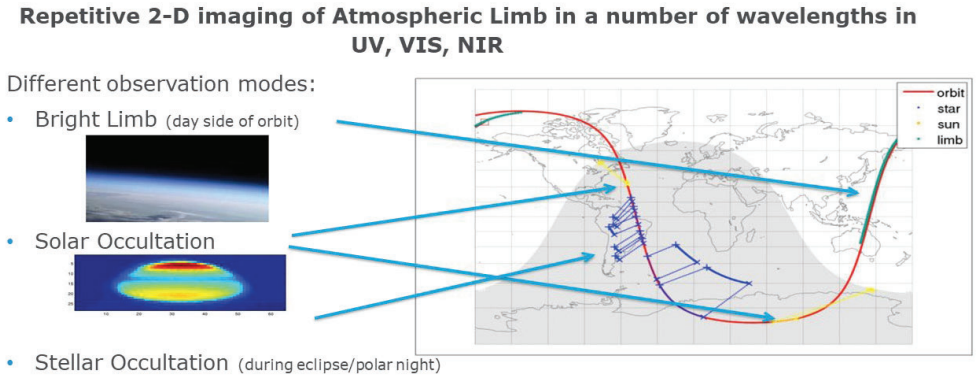

Figure 1 ALTIUS Mission Observation Modes

1.2 Platform

The ALTIUS platform is based on a PROBA-P-200 generation satellite – a small satellite weighting just 266 kg. The satellite flies in a Sun-synchronous orbit at an altitude of 668 km, achieving global coverage in a three-day revisit cycle. The P-200 platform, currently under development at QinetiQ Space, is an autonomous three-axis stabilised multi-purpose platform. It uses three star trackers, four reaction wheels, a GPS receiver and two GPS antennas, three magneto-torquers and two magnetometers. This ensures that the platform has a high degree of manoeuvrability for different observations, modes and operational scenarios. To meet the power needs of ALTIUS, four deployable solar panels will be accommodated on the platform. The Instrument for the mission will be mounted on top of the platform deck.

1.3 Ground Segment

The ALTIUS Ground Segment consists of the Flight Operations Centre (FOS), Payload Data Ground Segment (PDGS) and acquisition stations. The FOS is in charge of the satellite TT&C and will be located in the European Space Security and Education Centre (ESEC) in Redu (Belgium), making maximum re-use of existing infrastructure for the operations of the PROBA satellites. The PDGS provides all necessary functionality for mission planning generation, systematic and timely production, archiving and dissemination of Level 2 products for the primary objective and flexible ground segment processing and product delivery infrastructure in support of secondary objectives. The PDGS is expected to be installed in Belgian facilities in Uccle (Belgium).

2 ALTIUS INSTRUMENT

The ALTIUS Instrument consists of three independent spectral imagers capable of observing the atmospheric limb in the UV (250-355 nm), VIS (440-670 nm) and NIR (600-1020) nm. A distinct spectral tuneable filter element will perform observations in each of these three wavelength ranges, being an acousto-optic tuneable filter (AOTF) in the VIS and NIR and a setup of cascading Fabry-Perot interferometers in the UV.

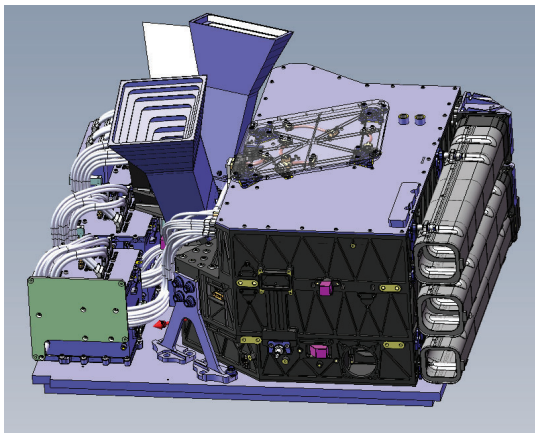

Figure 2. ALTIUS instrument optical unit and channels control units

2.1 Optical design

UV Channel:

The optical layout of the ALTIUS UV channel is described in Figure 3 and Table 1 and is based on an afocal optical layout integrating a cascade of 4 Fabry-Perot interferometers as spectral filter.

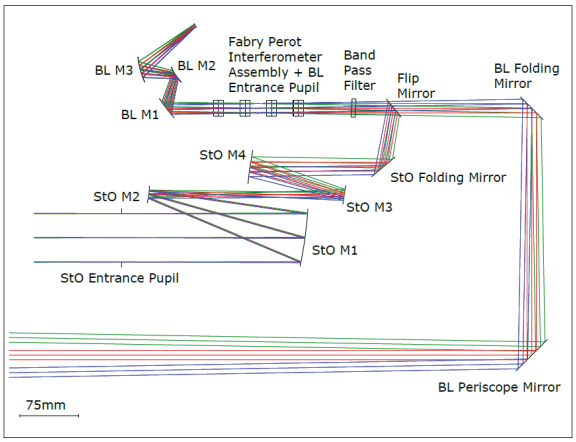

Figure 3 UV channel Optical design

Due to the low transmission UV spectral filter, limited by the maximum dimensions of the clear apertures of the FPI mirrors, it was necessary to have 2 distinct optical paths in the UV channel: the first one to perform bright limb and Solar occultation measurements and the second for stellar occultation. In the stellar occultation path, an increase of the effective SNR could be reached by coupling the FPI assembly with a 12 mm pupil to an entrance pupil of 62mm using a magnifying optical system at the expense of a reduction of the Field of view. The coupling between the optical paths is then done by means of a mechanism, which allows switching between the bright limb, the Solar occultation and the stellar occultation mode.

Table 1 Optical design first order properties of the UV channel

PARAMETER	UNITS	BRIGHT LIMB /SOcc	STELLAR OCC.
field of view	mrad	34 x 34	6.3 x 6.3
entrance pupil diameter	mm	12	62
total focal length	mm	106	568
StO optics magnification	mm	-	5.38
intermediate image size	mm	-	7.1 x 7.1
image size	mm	3.591 x 3.591	3.591 x 3.591

Other elements that form the UV channel are: the band-pass filter used to filter out any wavelength below or above the UV range of interest, the back-end optics to image the scene onto detector and the Focal plane assembly.

ALTIUS has very challenging straylight requirements in the UV which are difficult to manage in such instrument concept [1] [2]. One of the key targets for optimization is therefore the minimization of the scattering effect for each optical element. Therefore, all refractive optical elements are based on superpolished fused silica substrates while mirrors are based on Al RSA443 blank mirrors with a NiP polished plating. This ensures the micro-roughness is reduced within 1nm in the range between 1.5mm-1 and 1000mm-1. To prevent degradation on the initial substrate roughness, specific coatings are selected, and all elements are being monitored throughout the manufacturing process using white light interferometry and or BRDF measurements when possible.

VIS and NIR channels:

The optical layout of the ALTIUS VIS and NIR channel is described in Figure 4and Table 2. This is a confocal telecentric design based on an Acousto-Optical Tuneable filter (AOTF) as spectral filter. Both VIS and NIR channels are based on identical front end and back end mirror designs. The VIS and NIR AOTF are designed specifically for each wavelength range. A specific design of the front lens in each channel allows correcting the chromatic aberrations, induced by the AOTF's, specifically for each channel. This lens is defining the entrance pupils of the VIS and NIR instrument.

To account for the angular discrimination between the AOTF first and zero orders of diffraction it was necessary to restrict the pupil dimension in the VIS channel. This is not necessary in the NIR as the designers managed to ensure a sufficient angular shift between the two orders to be able to block the zero order directly by mechanical means.

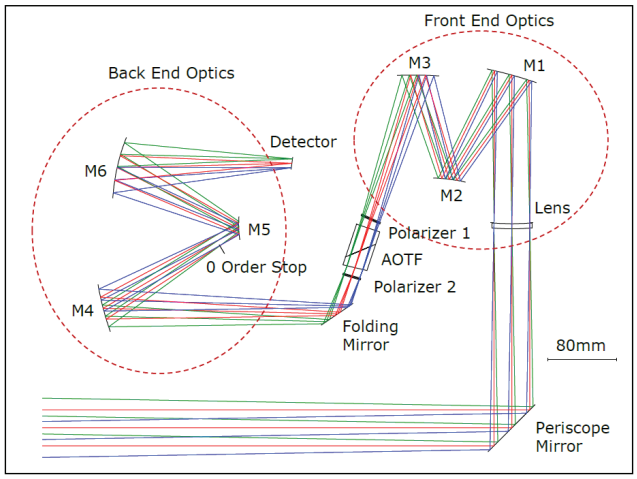

Figure 4 VIS channel optical design (the NIR channel has a similar design)

The VIS and NIR AOTFs are positioned in between cross oriented polarizers. These polarizers allow to constrain the input polarization entering the AOTF and to reject the light that is not diffracted by the AOTF, therefore reducing further potential zero order scattering contributions to the straylight performances.

Table 2: Optical design first order properties of the VIS & NIR channel

PARAMETER	UNITS	VIS	NIR
field of view	mrad	35 x 35	
entrance pupil diameter	mm	∅42 & 34.5x42	∅42
total focal length	mm	301	
front end optics focal length	mm	537	
intermediate image size	mm	18.8 x 18.8	
back end optics magnification		0.56	
intermediate pupil size	mm	11.4x17.6	13.7x17.7
image size	mm	10.521 x 10.521	

Similar to the UV channel, the VIS and NIR channel have a mechanism to switch between the observation modes, a back-end optic and the focal plane assembly. In these two channels the straylight requirements are again playing a large role in the requirements imposed on the different optical elements. The same approach as for the UV elements is, therefore. being followed.

3 TECHNICAL CHALLENGES

3.1 Fabry-Pero Interferometer Assembly

The design, manufacturing and test of the Fabry-Perot Interferometer Assembly is led by VTT in Finland. The design and optimization phase of the FPI assembly has been challenging and started by the need to trade-off conflicting requirements, the main ones are hereby being described:

- The FPI Assembly required throughput:

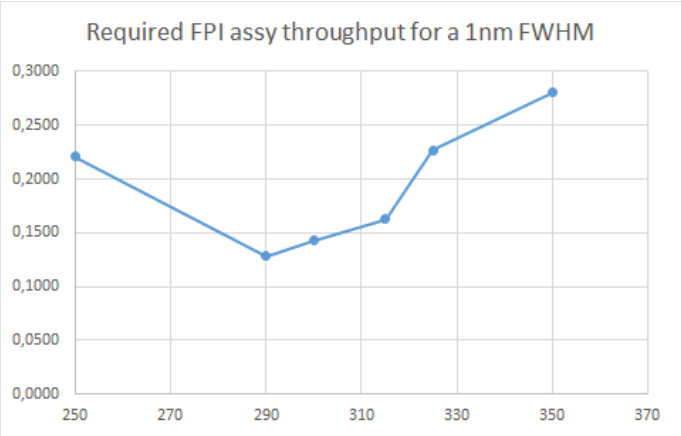

Figure 5 Fabry-Perot Assembly throughput requirement

- The FPI Assembly Maximum bandwidth:

Table 3: FWHM requirement for the UV Spectral filter

FWHM	Spectral range
10.0 nm	250 nm ≤ λ < 280 nm
5.0 nm	280 nm ≤ λ < 290 nm
3.0 nm	290 nm ≤ λ < 310 nm
2.5 nm	310 nm ≤ λ < 355 nm

- The FPI assembly out of band rejection:

$$\left(\int_0^{\lambda_C-8\text{nm}} SRF(\lambda)_{instrument} \cdot SRF(\lambda)_{FPI\ assy} \cdot SRW(\lambda_c,\lambda)\mathrm{d}\lambda + \int_{\lambda_C+8\text{nm}}^{\infty} SRF(\lambda)_{instrument} \cdot SRF(\lambda)_{FPI\ assy} \cdot SRW(\lambda_c,\lambda)\mathrm{d}\lambda\right) < \int_{\lambda_C-8\text{nm}}^{\lambda_C+8\text{nm}} SRF(\lambda)_{instrument} \cdot SRF(\lambda)_{FPI\ assy} d\lambda \quad (1)$$

The most relevant design drivers are described here below:

Number of FPI units: In order to have a performing system, the selection of a central wavelength needs to be done by a combination of several wavelengths. One of two units to select the central wavelength and the other to filter out spectral leak within the wavelength range of interest (see Figure 10). Also, a single FPI unit can be optimized to cover a small wavelength range, so in order to increase the wavelength range covered by the FPI assembly, the number of FPI units needs to be increased. The number of FPI units used will affect the main assembly requirements differently: using more FPI units will reduce the spectral leak but also reduce the throughput (more loss due to an increase numbers of mirrors).

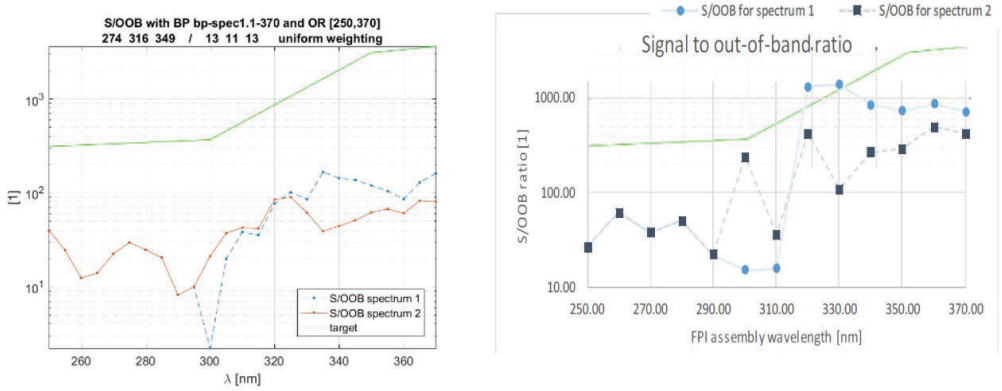

Figure 6 Example of Signal to out-of-band ration between an assembly with 3 FPI Units (left figure) or with 4 FPI units (right figure)

Number of layers in the FPI Bragg mirror coatings: Similar to the number of FPI units, increasing the number of Bragg mirror layers will reduce the spectral leak and lower the assembly throughput. Additionally, increasing the number of layers will reduce the FWHM.

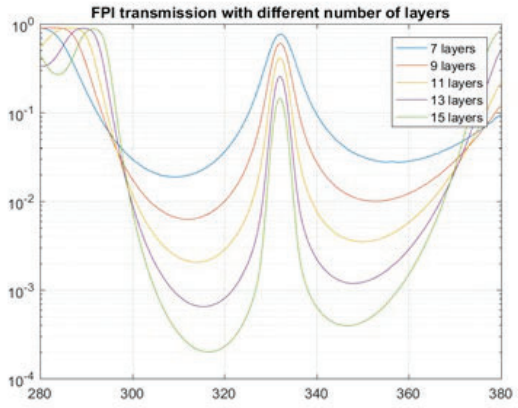

Figure 7 FPI transmission with different number of Bragg mirror layer showing a reduced transmission and a smaller FWHM with an increased number of layers

Manufacturing data: From a practical point of view, the main challenge remains in the limited amount of materials which can be used to produce UV-efficient dielectric coatings; leaving only HfO_2, MgF_2 and SiO_2 for the design optimization but also from the necessity to combine the need for a performing design with the necessity to have a robust approach with respect to manufacturability.

The use of manufacturing data to correlate with the model has been an important step toward the design of the flight coating. One of the important parameters is the complex index of refraction of Hafnium Oxide (HfO_2) used in the Bragg mirror coating. Variation of this refraction index during manufacturing has a direct impact on the FPI assembly performance indicators (FWHM, Throughput, Spectral leak). Finally, robustness of the optical design performance against mechanical tolerances had also to be considered to the benefit of manufacturability.

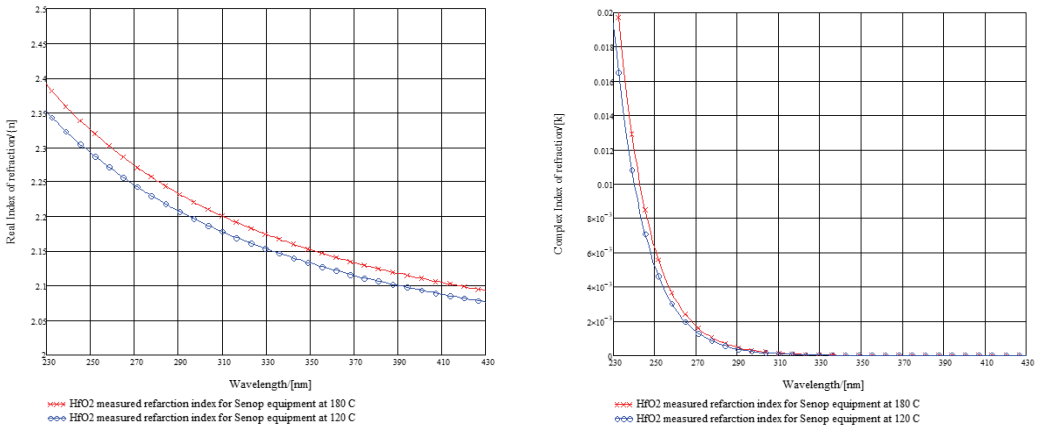

Figure 8 Real and complex refraction index of HfO2 as deposited

In order to design the FPI assembly, VTT has created a simulator that balances the different requirements using a pre-defined weighting factor. As described in Figure 9, there are a lot of interdependencies on the design parameters and furthermore, many of the design parameters are manufacturing dependent such as the mirror roughness or the mirror bending.

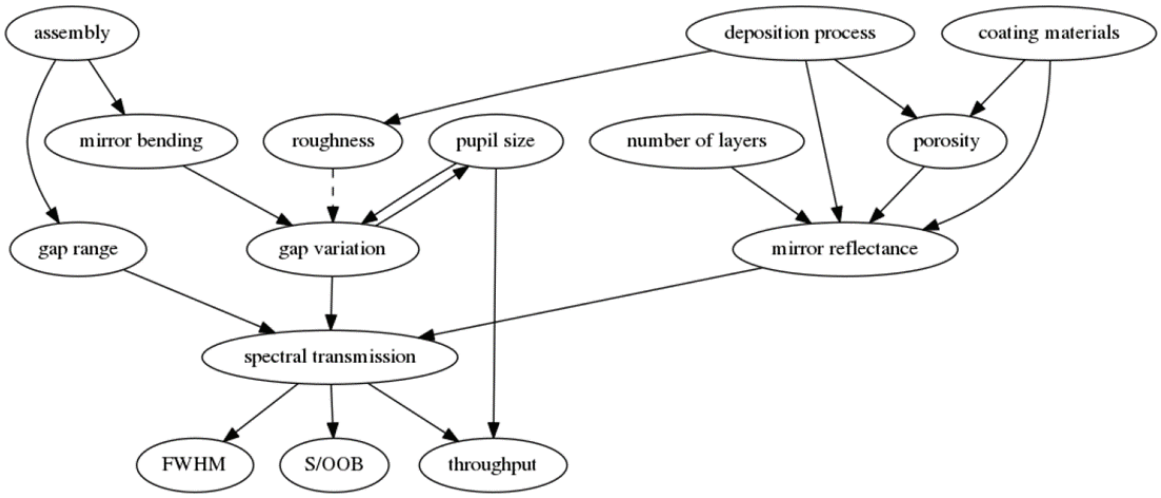

Figure 9: Extract of the FPI assembly design parameter interdependency

The final trade-off led to the following FPI assembly design:

Table 4 FPI Assembly design parameters

FPI	CWL [nm]	layers	tilt
1	257	9	−1.89
2	293	11	+1.89
3	328	9	−0.63
4	348	11	+0.63

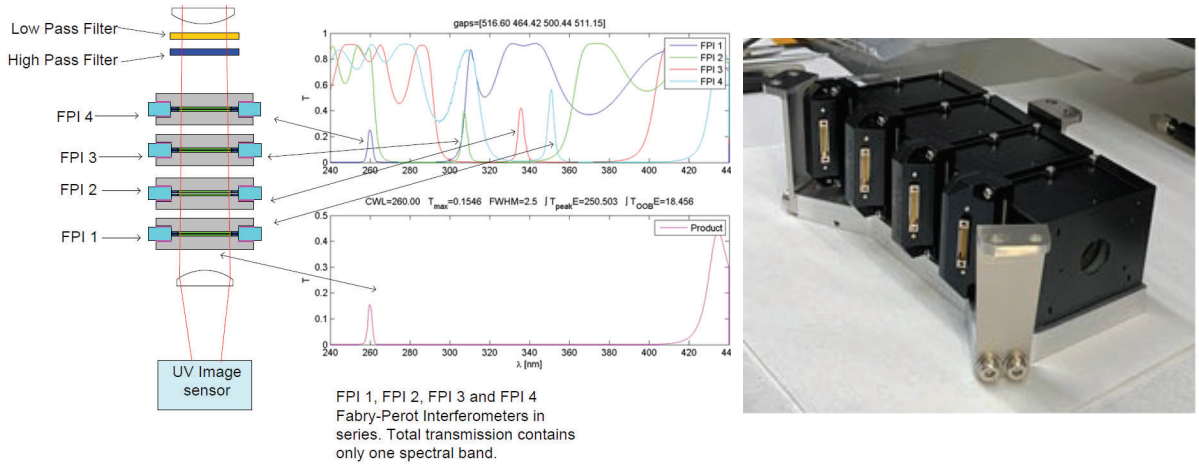

Figure 10 FPI assembly concept and example of an FPI assembly SRF for a central wavelength of 260nm

3.2 AOTF

In an Acousto-Optic Tuneable Filter (AOTF), the diffraction grating is created by acoustic waves traveling through the birefringent crystal. The acoustic wave is produced by a transducer bonded to the crystal, to which an RF frequency signal is applied. The frequency of the signal defines the selected wavelength.

The ALTIUS AOTFs are manufactured by Gooch and Housego. Several design drivers were taken into account during the iterative process to design the AOTF cells for the VIS and NIR channel. These parameters were mostly presented in [1].

Since the previous phase of development in 2020 and the progresses reported in [1]; the design approach of the large AOTF for the ALTIUS mission has been validated through a successful shock and vibration testing of a VIS AOTF EQM. This test campaign has also validated the design and performances of the custom double wire-grid polarizers developed with MoxteK which is planned to be used for flight.

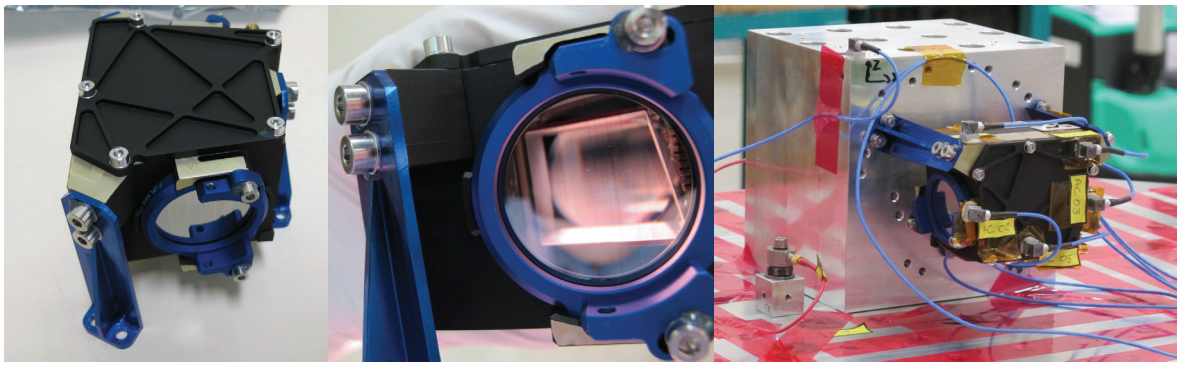

Figure 11 ALTIUS VIS pre-development AOTF.

In 2020 at the beginning of phase B2/C/D, the requirements on the AOTFs performances have been fine-tuned by the scientists for the VIS and NIR AOTF. The frequency range of the AOTFs have been narrowed down from respectively 400 – 800 nm to 440 – 670 nm in the VIS range and 900 – 1800 nm to 600 – 1020 nm in the NIR range. In the same time the spectral resolution required had been increased to a maximum bandwidth of 1.4nm at 440nm and 6.82nm at 1020nm in order to enhance detection capabilities of other scientific species of interest.

As such the design of both VIS and NIR AOTF cells had to be fully redone with new AR coatings and an updated thermo-mechanical design. The news designs are fitting to the science requirements in both wavelength ranges as can be seen in Figure 12.

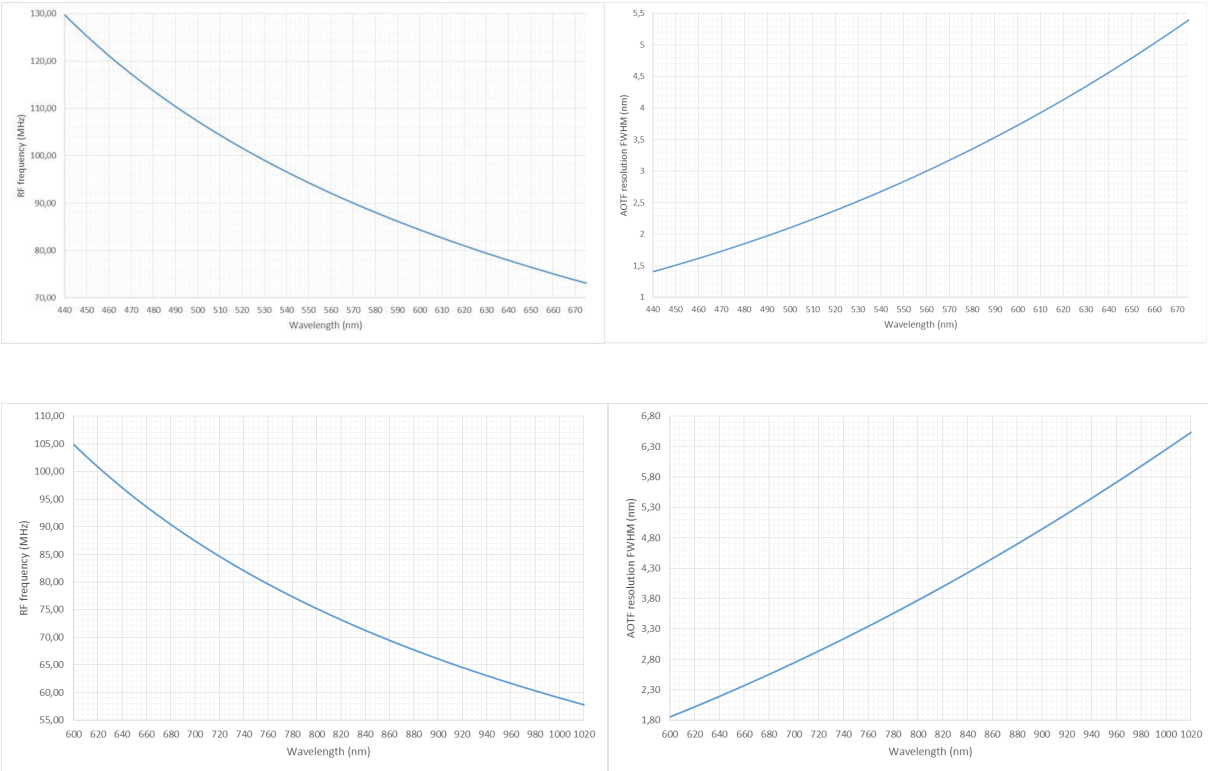

Figure 12 : Top: VIS AOTF wavelength to RF frequency and resolution performances Bottom: NIR AOTF wavelength to RF frequency and resolution performances

Nevertheless, the newly achieved compliance has come at the expense of more technical challenges, such as:

- The operating RF frequency range of both cells increased significantly. As a consequence, the dimensions of the piezo transducer necessary to transfer the RF to the AOTF crystal, and in particular their thickness, had to be reduced significantly bringing piezo bonding and polishing as a quite critical aspect to master during the manufacturing activities. This aspect introduced multiple failures during the manufacturing process reducing severely the yield of the production, which is still ongoing for all EM, QM and FM at the moment of writing this paper.
- The AOTF crystal dimensions have increased significantly, leading to a redesign of the housing of the crystal introducing the need for a re-qualification of the AOTF assembly for the project.
- The separation angle for the zero and first diffracted order, in particular in the VIS channel, could not be maintained large enough such that a direct separation of the two orders could be made only by mechanical means. As a consequence, this led to the need of artificially reducing the entrance pupil of the VIS Channel to prevent order overlap allowing proper zero order rejection. This reduction combined with narrowed resolution while still maintaining a high SNR requirement has led to increasing needs to develop high performance coatings.

3.3 Optical elements and coatings

Besides the spectral filters, the mirrors and the optical coatings are the critical elements needed to reach the performance requirements.

Coatings:

In the UV channel; OIP commissioned, during phase B of development, Optics Balzers to design, manufacture and qualify a UV band-pass filter which could provide very good transmission over the UV range of interest (250nm-355nm), very sharp rising and cutting edge and excellent extinction ratio up to 1000nm wavelength. This development was by itself a technical challenge as the design was composed of:

- 386 layers HfO2/SiO2 on face one; which defines the pass-band and the blocking range until 700 nm;
- 318 layers of the same materials on face 2; which defines the blocking from about 700 nm to 1000 nm
- For each layer, the typical layer thickness was ranging between 10 nm and 100 nm.

Furthermore, in order to reach the requirements, it was proven during the pre-development that a final oxidation of the layer, achieved throughout a heat treatment, was necessary to achieve high transmittance within the passband. Despite technical challenges this development successfully led to a flawless qualification.

Nevertheless, in 2020, the extensive QE testing of the CIS115 sensor planned to be used for the mission revealed more sensitivity than simulated in the NIR and deep UV. This observation combined with the consolidated spectral leakage performances of the optimized FPI assembly led to identify the need for extending the blocking band of our bandpass filter to 1200nm and sharpen the rising edge of the transmission band to 245nm instead of 250nm.

This led to a new design iteration with an additional increase of design complexity and thicker coating layers than originally planned:

- 478 layers HfO2/SiO2 on face one; which defines the pass-band and the blocking range until 700 nm;
- 332 layers of the same materials on face 2; which defines the blocking from about 700 nm to 1200 nm
- For each layer, the typical layer thickness was ranging between 10 nm and 100 nm.

As part of the new development the heat treatment was pushed to a higher temperature to achieve the required transmittance between 245 and 250nm. Unfortunately, this treatment revealed cracks in the coating. A study was put in place in order to maximize the performance with a lower bake-out temperature. The results of this study led to the filter performance plotted in Figure 13, which are very close from the requirements in the band edges and exceed them in the main transmission band.

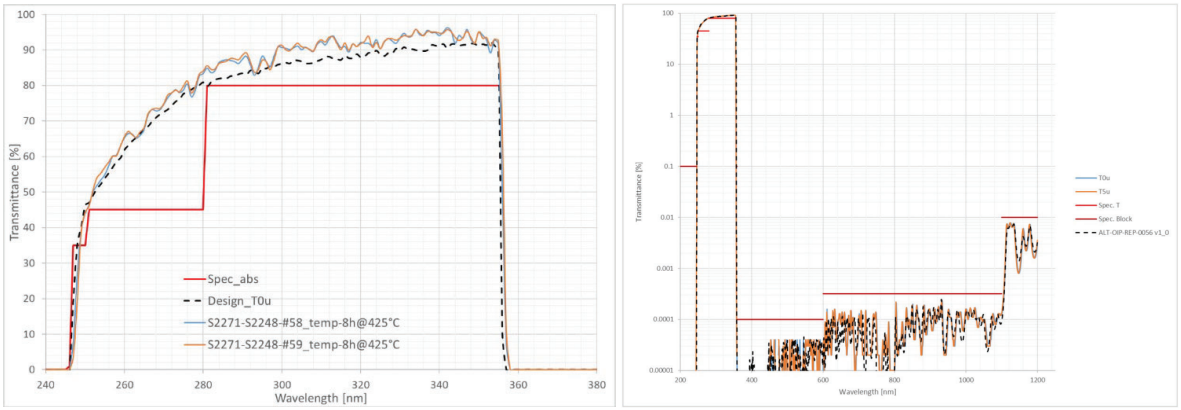

Figure 13 : UV bandpass filter design to as build performances in the transmission band and in the blocking band

To further improve the out-of-band rejection in the UV channel, “cold mirror” coatings were implemented on the UV mirrors. These coatings are made by depositing on the NiP plating of the mirrors. First a black titanium layer followed by a dielectric coating is applied with the aim to reduce the reflectivity at higher wavelengths and act as a low pass filter. The development of the coatings for this “cold mirror” is still under qualification, despite the fact that their spectral performances are excellent, the measurements made under white light interferometry revealed that the nominal used process was worsening the mirrors roughness in an unacceptable manner, going from about 1.2nm within the required frequency range to 4nm. This coating was made of first Ti layer deposited by IAD (Ion Assisted Deposition) followed by the dielectrics layers (Ta and Hf deposited by IAD).

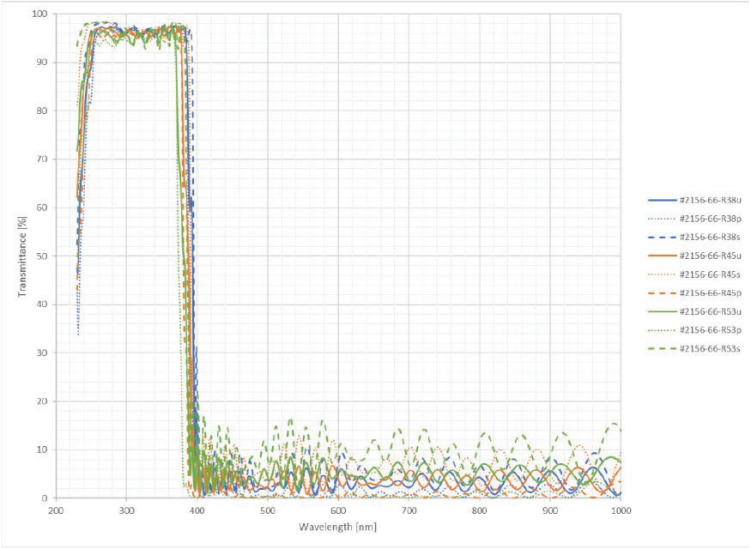

Figure 14 : Measured reflectance for an ALTIUS cold mirror as part of the qualification activities

In order to improve the roughness, two updated coatings recipes based on lessons learned from past space projects are under testing at the moment of writing the paper.

Table 5 Updated Cold Mirror coating recipe

Recipe 1	Recipe 2
• Ti layer deposited by PARMS • Ta layer deposited by PARMS • Hf layer deposited by IAD	• AL layer deposited on the substrate before the cold coating • Ti layer deposited by PARMS • Ta layer deposited by PARMS • Hf layer deposited by IAD

One of the main differences was the use of Plasma Assisted Reactive Magnetron Sputtering (PARMS), instead of IAD. Furthermore, the second recipe added an aluminium layer to act as a barrier between the substrate and the coating. Current roughness measurements, after the deposition of the Ti black coating for both samples, showed that recipe 2 gives good results, whilst for recipe 1 a clear dotted pattern resembling a cheetah skin is observed (see Figure 15). The remaining steps of the coating- and qualification activities will be based on this second coating recipe.

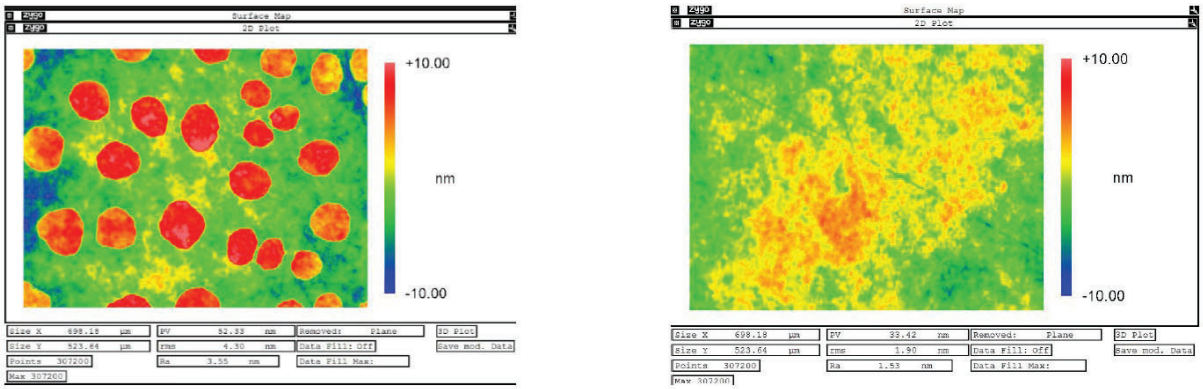

Figure 15 White light interferometry results of the 2 black coating recipe trial: On the left, results of the receipt 1 showing the cheetah pattern and on the right the results of the receipt 2 that used an additional Al layer as barrier between the substrate and the coating

3.4 Straylight

The principal science goal of the ALTIUS mission is to retrieve the vertical profile of stratospheric Ozone. The vertical stratification is obtained by observing the Earth's limb tangentially to its surface. This means the bottom part in a single image samples the Earth's atmosphere near 0 km above the surface whereas simultaneously the top part of the image samples the atmosphere 100 km above the surface (see Figure 1). The signal captured by the instrument is, in first instance, light scattered by the Earth's atmosphere, thus the received signal drops six orders of magnitude depending on the wavelength as the atmosphere rarefies with height (see black line in Figure 16).

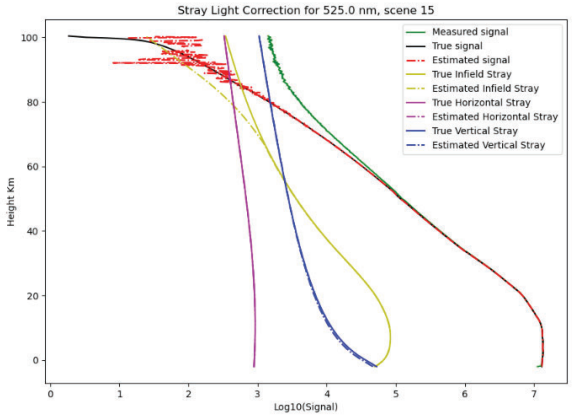

Figure 16 Breakdown of signal contributors versus altitude expected in a typical ALTIUS vertical profile

The rapid drop in direct signal entails, amongst other problems, straylight. Even though the central peak of the PSF contains >80% of the power (see Figure 17), the fall-off atmospheric limb signal even just within the observed FOV is comparable to the fall-off of the PSF wings. Once scattered light outside of the observed FOV is considered, in particular light reflected by the Earth's surface, the true signal falls-off more rapidly than the straylight. Typically, the stray light dominates over the true signal from altitudes above 60 km depending on wavelength, as shown in Figure 16 by the green and black lines.

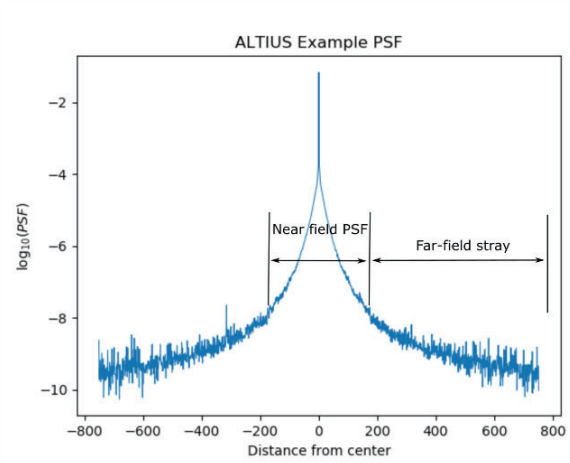

Figure 17 A typical PSF used in the ALTIUS mission. The UV PSF would also contain laterally off-set ghosts as per instrument design.

In the VIS and NIR Channel, the straylight is dominated by in-field straylight at low altitudes and near out of field (NOoF) straylight (from the 0-order light passing through the AOTF) at high altitudes. The main contributor to in-field straylight is scattering and ghosts. In all channels, state-of-the-art single point diamond turned Al mirrors with a polished nickel plating are used. Those mirrors have a roughness requirement of approximately 1nm rms. Improving this aspect is very challenging while the optical design remains refractive based. Contamination is another source of scattering (for this purpose a contamination level of 600ppm is used). This level is high but based on realistic AIT budgets. The angles of the different optical surfaces, mainly the AOTF surfaces, and their tilt with respect to the polarizer have already been optimized to reduce ghosts.

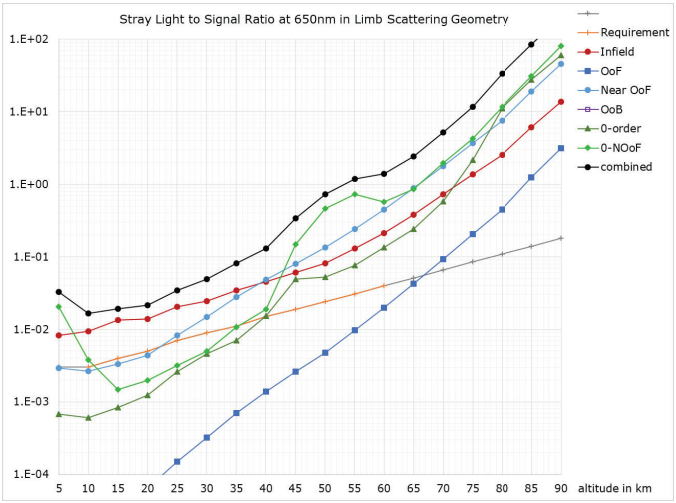

Figure 18 Straylight per contributor in the VIS channel at 650 nm

In the case of Near OoF straylight, several analyses have been executed to identify the main contributors and assess possible solutions to reduce these. Raytracing analysis indicated than 25% of the contribution of the total scatter comes from the first optical element, the periscope mirror. In an attempt to reduce this contribution simulations were done using a glass periscope mirror in order to reduce the roughness of this element. The gain of this measure was not sufficient to counterbalance the impact on the instrument development plan (see Figure 19). A theoretical exercise of having "perfect Mirrors" was also performed for comparison. This of course led to a more significant improvement but only indicates a theoretical best case.

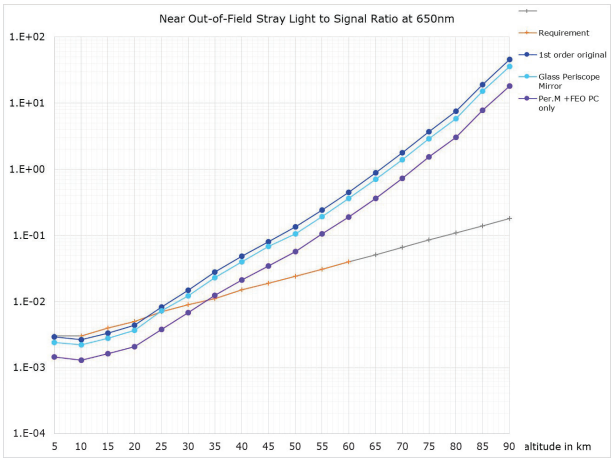

Figure 19 VIS Near Out-of-File straylight analysis with reductions measures.

The zero order straylight coming out of the AOTF is mainly blocked by the polarizers and a field stop at the level of the back-end-optics. However, both in the VIS and in the NIR extra measures have been added to reduce the 0-order contribution. In the VIS channel, the addition of a field stop at the exit of the AOTF shows improvement (Figure 20). This extra field stop is only useful in the VIS channel as the separation angle between the 0-order and 1st-order of the VIS AOTF is low (see section 3.2).

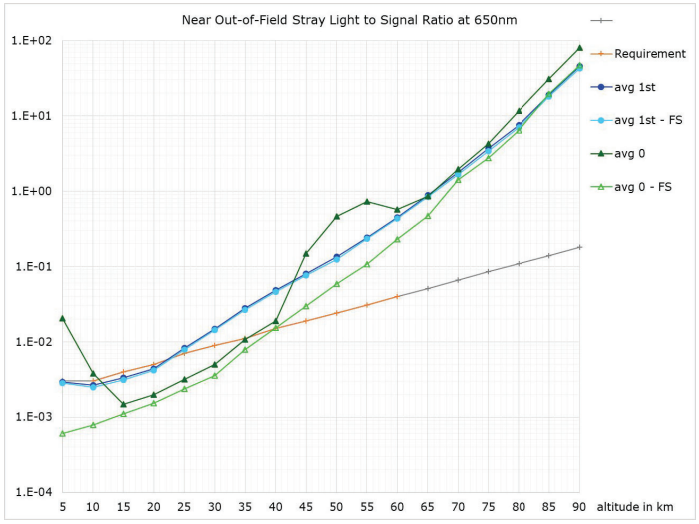

Figure 20 VIS 0-order straylight with and without the additional Filed Stop (FS)

In the NIR channel, due to the QE profile of the CIS115 sensor, the addition of a band-pass filter on the lens of the front end optics also reduces the straylight contribution as it blocks, before spectral filtering by the AOTF, a large part of the unwanted spectrum (outside of 600-1020 nm range). This extra band-pass filter is only useful in the NIR channel as the QE of the detector is much higher in the VIS range than in the NIR range (Silicon based detector) and therefore 0-order straylight in the VIS range would have higher weight when converted to electrons than the desired signal in the NIR range.

Figure 21 Schematic impact of a bandpass filter in the NIR channel and QE of the detector with respect to the NIR band

In the UV channel, the straylight is dominated by in-field straylight and also Near OoF straylight for higher wavelengths (350nm). As for the VIS and NIR channel, the use of state-of-the art mirrors for roughness has been implemented to reduce scattering. However, the UV spectral filter is a combination of 4 Fabry-Perot interferometers, each having 4 optical surfaces. The total amount of optical surfaces, including the mirrors and bandpass filter, adds up to 23 surfaces in total which explains the strong impact of in-field straylight. In an effort to reduce ghosts a tilt of the individual FPI with respect to each other has been implemented (see Table 4). The ghost reduction is mainly important along the vertical direction as the goal of ALTIUS is to retrieve the vertical profile of the Ozone and error in the vertical signal will directly affect this product.

Near OoF straylight is only dominant for higher wavelengths at it is coming from the earth albedo, whilst the earth atmosphere filters most of the lower UV wavelengths.

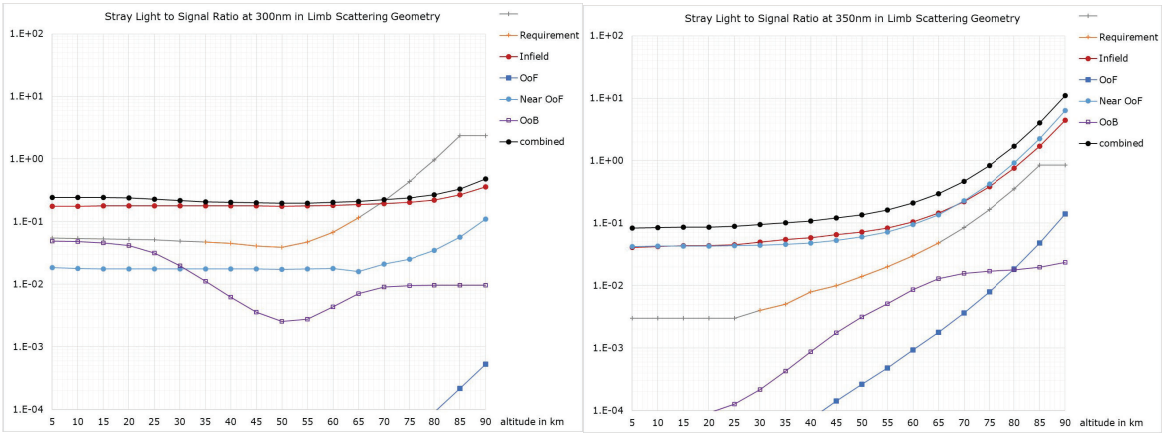

Figure 22 UV channel straylight curve for 300nm and 350nm

3.5 Structural and Thermal design

The NIR-channel and the VIS-channel are both accommodated in the same H-shaped structure. This part, the primary optical bench, is physically the largest and the heaviest piece of the instrument's infrastructure. The structure of the optical unit is made of Aluminium 7075-T7352. The UV-channel is accommodated in a shallower U-shaped structure. This secondary optical bench is mounted onto the bottom-side of the primary optical bench. The other optomechanical elements are also made of Aluminium in order to minimize any thermo-elastic deformation and ensure that the optical performances are kept stable throughout the duration of the mission.

The thermal design of the instrument, focussing on six main active components (one filter and one detector per channel), consists of cold-biased heat rejection mechanisms (radiator, thermal straps) which are dimensioned for hot operational cases. The remaining internal active sub-units such as the mechanisms or housekeeping electronics have no dedicated thermal control but are (mechanically and) thermally coupled to the optical unit. The feasibility of this passive thermal design has been demonstrated by analysis, where temperature variation across an orbit remains minimal below 1°C ensuring a good thermal stability. The temperature variation over seasons and the lifetime is however larger, imposing the need for qualifying the instrument and subsystem over an operational temperature range of -40°C to 55°C.

3.6 Contamination control

As any optical mission, the ALTIUS instrument is sensitive to particulate contamination, which increases the scattering of the light. Furthermore, ALTIUS also has a UV channel which makes it particular sensitive to molecular contamination. Indeed, molecules outgassed from the different materials within the instrument will redeposit on the surfaces, including optical surfaces. Exposition to UV radiation polymerizes those molecules which then become permanently fixed onto the surface, ultimately reducing its optical properties.

In ALTIUS, special measures are taken in order to reduce the amount of contaminants (both molecular and particulate) and mitigate their impact. Those measures affect the design, MAIT and operations of the Instrument.

First, from a design point of view, the potential outgassing sources have been removed, to a maximum extent from the optical benches of the Instrument. The electronics are placed in separate boxes outside the benches. Glues, especially silicone based, are not used if not strictly necessary. Dedicated purging lines have been designed into the optical bench to ensure that purging can be done optimally for the critical elements (detector, spectral filters) and dedicated heaters are placed to allow for in-flight decontamination.

From a MAIT perspective, bake-out of all items, use of cleanroom facilities, dedicated cleaning procedure and constant purging with dry nitrogen is applied to limit the contamination during this phase. The purging is even kept up to the last day before launch, while the satellite is already inside the rocket fairing.

During operations, specific constrains are given to ensure that the Sun does not enter the FoV of the instrument during the first 4 weeks after launch to ensure that proper outgassing can take place. Furthermore, the decontamination heater can be

used to raise the local temperature of the critical elements (Detector and Spectral filter) in order to outgas molecular contamination that would deposit on those surfaces.

Finally, all those measures are supported by simulation using the ESA development software FCMT which allow to qualitatively assess the impact of the measures taken.

4 INSTRUMENT PERFORMANCE

4.1 Straylight correction

Given the challenging observation conditions, meeting the ALTIUS stray light requirements demands the addition of an extra post-image-acquisition processing step to specifically reduce the stray light within the image. The University of Saskatchewan has developed this processing step and it takes the form of an elaborate PSF deconvolution. Typical deconvolution problems have a PSF which is smaller than the measured image, and the quality of the deconvolution result is principally determined by PSF knowledge, noise, and chosen deconvolution method. However, in the case of ALTIUS we noted that stray light originating outside of the measured FOV makes a significant contribution total measured stray light. This leads to the additional problems that the PSF needs to be known to an extend larger than the measured FOV and the scene next to the FOV needs to be estimated.

The problem can be divided into a vertical and horizontal component. The vertical component is the most difficult since the reflectivity of the Earth is highly variable and is solved by using a high-altitude proxy. Figure 16 shows that the vertical stray light is the dominant component in the highest altitudes by more than an order of magnitude. It is estimate using a low-order polynomial fit the observed profile and in combination with a given PSF the radiance reflected by the Earth's surface can be estimated. Stray light coming from the out-of-FOV can be approximated by assuming the scene is horizontally invariant and extending the PSF by fitting a Harvey curve to its outer wings. The final true input signal is then estimated iteratively whereby the vertical stray-light is first subtracted from the measured signal followed by a deconvolution to remove the PSF contribution within the FOV and out of the FOV in the horizontal direction.

The algorithm is able to remove the stray light effectively enough to meet the ALTIUS stray light requirements as is demonstrated in Figure 23. Note, that the deconvolution process reduces the SNR of the final output as expected (compare green and red line in Figure 16). Furthermore, the straylight removal algorithm is not able to remove stray light if the input signal is low as seen in the higher altitude in Figure 23.

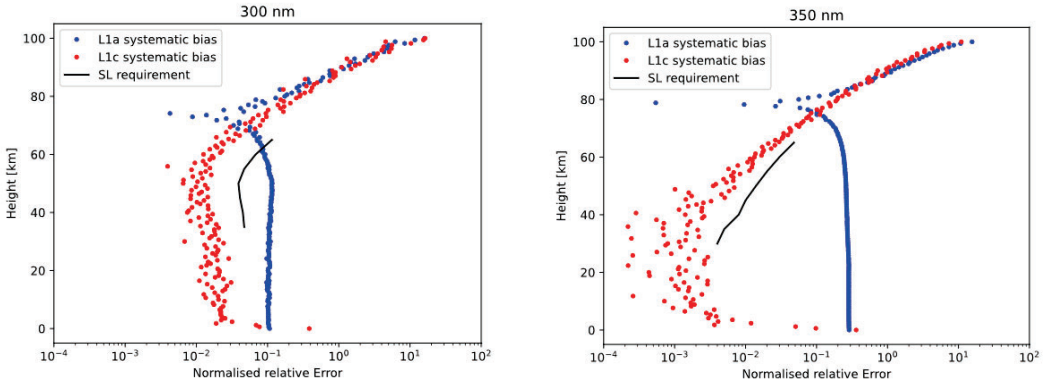

Figure 23 Straylight reduction algorithm results for 300nm (left) and 350nm (right) by PSF deconvolution done in the System Performance Simulator (SPS).

Note that, the PSF knowledge is a key requirement in order to perform an adequate stray light removal which in turn has prompted the monitoring and assessment of particle contamination as well as dedicated in-flight PSF calibration campaigns.

4.2 Spectral Rejection

As discussed in the section 3.3, a lot of effort have been made in developing dedicated coatings in the UV channel, both for the Band-pass filter and the mirrors. Behind this development is the need of excellent spectral rejection in order to limit Out-of-band straylight which is dominant in the case of Stellar occultation.

In the Figure 24, results of the stray light ration for star with a black body temperature of 3000k is shown for the PDR design of the UV channel and after the implementation of an improved UV band-pass filter and of the cold mirror coatings. Looking at the 300nm curve, the benefit from those coatings on the spectral rejection performance is obvious. This improvement in the UV channel permits the use of more stars for Stellar occultation measurements.

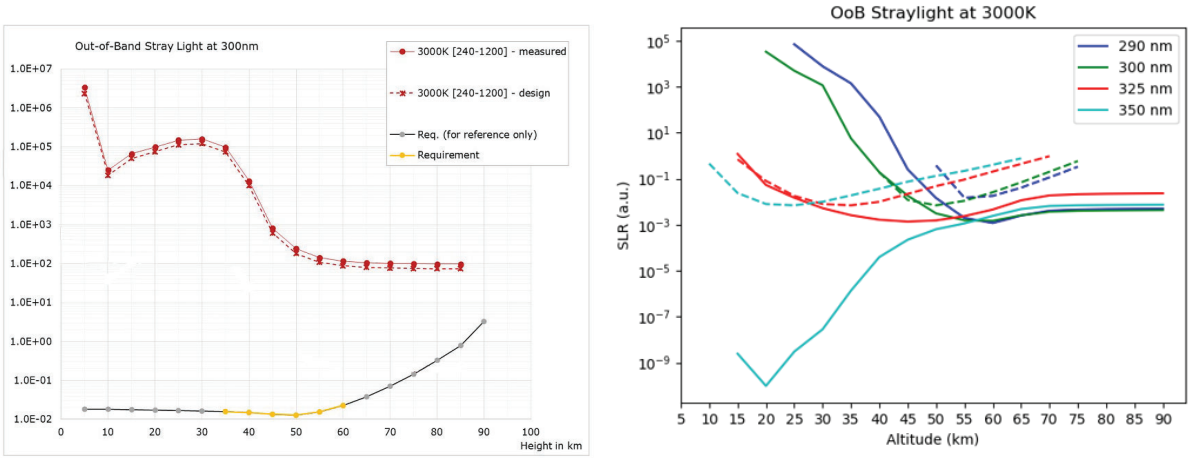

Figure 24 Out-of-band straylight ration for a star with black body temperature of 3000k: Left, PDR results for 300nm, right, results after improvement of the UV bandpass filter coating and implementation of cold-mirror coating.

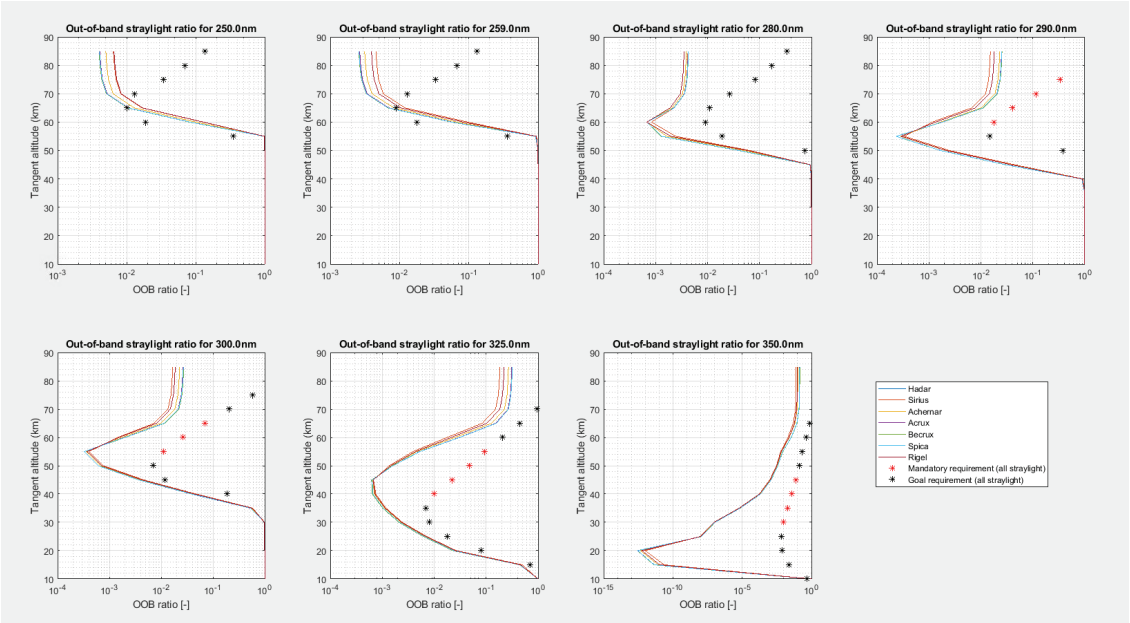

Figure 25: Out-of-Band ration in the UV channel for the 7 Stars that can be imaged

5 CONCLUSIONS

This paper has provided an overview of the technical challenges characterizing the development of the ALTIUS Instrument. The main novelties are linked to the spectral filters in all three channels of the Instrument: the Fabry-Perot Interferometer Assembly for the UV channel and the Acousto-Optical Tuneable Filter for the VIS and NIR channel. For both filter types, the complex trade-off was necessary to reach the designer performances presented. This trade-off led to the use of a cascade of 4 FPIs in the UV channel in order to reach the necessary Out-of-Band rejection in combination with an increased aperture for Stellar occultation, to reach the necessary SNR require for science data retrieval. In the VIS and NIR channel the design of the AOTF reaches the fabrication limits to satisfy the spectral requirements of ALTIUS which led to an increased manufacturing complexity and low production yield.

The results of the optical coatings development are shown with particular attention to the UV mirror coating and UV band pass filter coating. In both cases, the development is still ongoing at the time of writing this paper. The UV band-pass filter has developed cracks after heat treatment and, although a stable recipe is under qualification, the results are not yet confirmed. For the UV mirror coating, the main problem arises in the roughness that does not meet the ALTIUS requirements of < 1nm RMS. Here, parallel tests of different recipes have led to the identification of a good candidate which is also under-going qualification at the time of writing.

Finally, the paper has given a snapshot of other challenges, related to stray light and contamination, and the efforts put in place to correct straylight effects at L1 level using a deconvolution algorithm. This algorithm showed that straylight contribution could be reduced to within requirement, also in the case where contamination level used by the algorithm is different than the real contamination level.

ESA acknowledges the contribution and collaboration of the ALTIUS Mission Prime (QinetiQ Space N.V.), of the ALTIUS Instrument Prime (OIP N.V.) and of all their Subcontractors and Suppliers involved in the ALTIUS Instrument development.

REFERENCES

[1] L. Montrone et al. Proc. SPIE 11151, Sensors, Systems, and Next-Generation Satellites XXIII, 111510S (2019)
[2] J. Moreno-Ventas et al, ALTIUS Instrument: A study of scattering effects, This conference
[3] https://www.esa.int/Applications/Observing_the_Earth/Altius , ALTIUS web page